Short Communication

One-Step Synthesis of Co@C Composite as High-Performance Anode Material for Lithium-ion Batteries

Ming-Jun Xiao[1], Fu-Liang Zhu[1,3], Gong-Rui Wang[1], Chao-Yu Duan[1], Yan-Shuang Meng[1,3,] and Yue Zhang[2,*]*

[1] School of Materials Science and Engineering, Lanzhou University of Technology, Lanzhou 730050, China
[2] Department of Mechanical and Industrial Engineering, Texas A&M University-Kingsville, Kingsville, Texas, 78363, USA
[3] State Key Laboratory of Advanced Processing and Recycling of Non-ferrous Metals, Lanzhou 730050, China
[*]E-mail: mengyanshuang@163.com, yue.zhang@tamuk.edu

A carbon-coated cobalt (Co@C) composite was synthesized by a one-step method using ionic liquid as carbon source and reducing agent. The Co@C composite exhibited a core-shell structure, in which the cobalt nanoparticles uniformly embedded in the carbon matrix. When used as the anode material for lithium ion batteries, the cobalt nanoparticles enhanced the kinetics of Li+ and electronic transport during the charge/discharge process. The Co@C composite material delivered a reversible capacity of 657.3 mAh g^{-1} after 60 cycles at a current density of 0.1C and exhibits improved rate performance when compared with pure carbon.

1. INTRODUCTION

With the increasing challenge of environmental pollution and energy crisis, green energy has become the research focus in the world. Lithium-ion batteries (LIBs), as a new type of clean rechargeable power supply, possess the advantages of high voltage, high specific capacity and no pollution. High reversible capacity, high rate performance and good cycle stability are required when LIBs are used in large-scaled energy storage, such as electric cars, and large equipment[1-5]. The anode material is one of the most important factors that influence the performances of LIBs. Currently, the commonly used anode materials are graphitic carbon materials which have high cycle performance and rate performance. However, the low specific capacity (372 mAh g^{-1}) restricted the application of

graphitic carbon in the energy storage for large-scaled device [6]. It is necessary to develop new anode materials with high specific capacity, rate performance, and cycle stability.

In order to improve the specific capacity of carbon anode material, some researches have been carried out to synthesize porous carbon or metal-oxide/carbon composites[7]. It is found that the carbon composites with transition metals or transition metal oxides exhibit better electrochemical performance than pure carbon materials[8-11]. The introduction of transition metals not only enhances the specific capacity, but also improves the rate performance of carbon anode material. Mai et.al synthesized graphene-Ni hybrid material and found that the anchored nickel nanoparticles could increase the electrical conductivity and also modify the structure of SEI film covering the surface of graphene[12]. The Co@C composite exhibited improved electrochemical performance due to the transition metal, cobalt, which can enhance the electrical conductivity of electrode and catalyzed the lithium-carbon reaction in the electrochemical processes [13].

Herein, an one-step method is used to synthesize Co@C composite, using ionic liquid 1-butyl-3-methylimidazolium dicyanamide ([BMIm]N(CN)$_2$) as carbon source and cobalt acetate (Co(AC)·4H$_2$O) as cobalt source. The structure characterization results show that cobalt nanoparticles are embedded in the carbon matrix providing an integrated conductive network. The electrode materials are then assembled into a half-cell to measure the electrochemical performance. Due to the catalytic activity of cobalt nanoparticles and the integrated conductive network, the prepared Co@C composite exhibits a higher reversible capacity, better rate performance and less hysteresis than carbon matrix. These results indicate that Co@C composite is a promising electrode material for LIBs, which would be suitable for widespread applications.

2. EXPERIMENTAL

2.1 Materials Preparation

The carbon source ([BMIm]N(CN)$_2$, 2 g) and cobalt source (Co(AC)·4H$_2$O, 1 g) were first mixed and ground. The mixture was then transferred to a tube furnace purged with argon gas. The mixture was heated to 350 $^{\circ}$C and kept for 0.5 hour, followed by heating to 650 $^{\circ}$C and kept for 1 hour. The materials after heating were collected and denoted as Co@C. Pure carbon material was prepared as control and denoted as C, which was produced through the same procedure without cobalt source.

2.2 Material Characterization

The pattern of powered X-ray diffraction (XRD) was collected by using a Rigaku D/MAX 2500 V X-ray diffractometer with filtered Cu Kα radiation. The transmission electron microscopy (TEM) was performed on a JEOL JEM-2010F equipment. Raman spectra were recorded on a LabRAM HR UV/vis/NIR (Horiba Jobin Yvon, France) with a CW Ar-ion laser (514.5 nm) as an excitation source. Fourier transform infrared (FT-IR) spectra were recorded on a Nicolet-670 (America) spectrophotometer.

2.3 Electrochemical measurement

Electrochemical measurements of the anode materials were performed in a coin-type cell. The anode electrodes were fabricated by using 70% active material, 20% Super P, and 10% polyvinylidene fluoride in N-methyl pyrrolidone to form slurry. The slurry was then coated onto a Cu foil. The solvent was evaporated in vacuum at 80°C for 12 hours. A lithium foil counter electrode was invoked. A Celgard 2400 micro-porous polypropylene film was used to separate electrodes. The electrolyte was prepared by dissolving 1 M lithium hexafluorophosphate ($LiPF_6$) in a mixture of ethylene carbonate (EC) and diethyl carbonate (DEC) with a volume ratio of 1:1. Nickel foam was used to support the battery shell. Coin cell was assembled inside a glove box filled with dry argon. The charge-discharge tests were performed on a battery test system (Land CT2001D, China). Electrochemical impedance spectra (EIS) and cyclic voltammetry (CV) measurements were carried out at room temperature on a CHI660D electrochemistry workstation (Huachen, China).

3. RESULT AND DISCUSSION
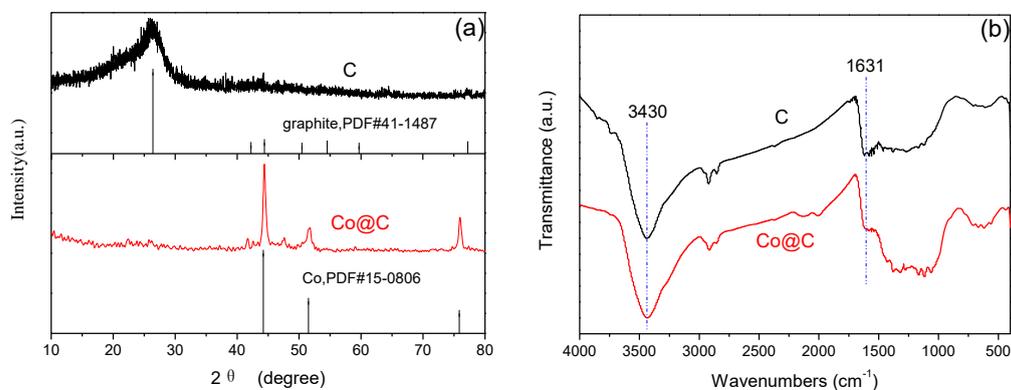
Figure 1. XRD patterns (a) and FTIR spectra (b) of the Co@C and C

Figure 1(a) shows the XRD patterns of Co@C and C. In the pattern of Co@C, the peaks at 2θ= 44.7°, 51.8° and 76.8° are characteristic peaks of metallic cobalt (PDF15-0806)[14]. The size of cobalt particle is 28 nm, calculating by using Scherrer's formula. In the pattern of C, the broad peak at around 25°corresponds to the (002) plane of graphite. The FTIR spectra of Co@C and C are shown in Figure 1(b). The absorption peak at 3430 cm^{-1} are ascribed to –OH of water existed in samples or KBr [15]. The broaden absorption between 1000 cm^{-1} and 1700 cm^{-1} is attributed to the stretching vibrations of graphitic carbon ring. The peak at 1631 cm^{-1} corresponds to the C≡C of carbon materials in both Co@C and C[16]. The FTIR result shows that the chemical structure of carbon materials is not changed by the integrated cobalt nanoparticles.
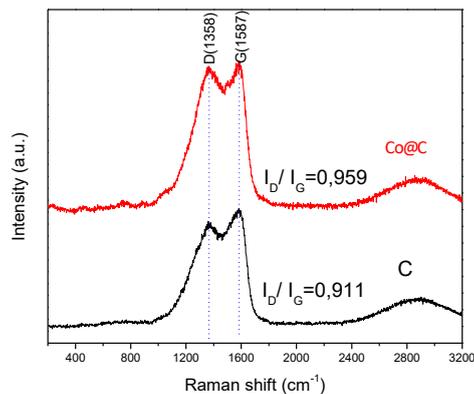
Figure 2. Raman spectra of Co@C and C

Figure 2 shows the Raman spectra of C and Co@C samples. Two characteristic peaks of D-band (1358 cm⁻¹) and G-band (1587 cm⁻¹) are clearly observed, indicating the presence of graphite carbon in both samples. There is a notable shift in the D and G bands of Co@C sample. This shift indicates the presence of large amount of disorders in the carbon planes of the graphitic carbon in Co@C[16]. The disorder degree of graphite crystal structure of carbon materials can be characterized by the intensity ratio of G band and G band. The I_D/I_G ratio of Co@C is nearly 1, indicating a large number of defects , which is beneficial for electrochemical properties[17].
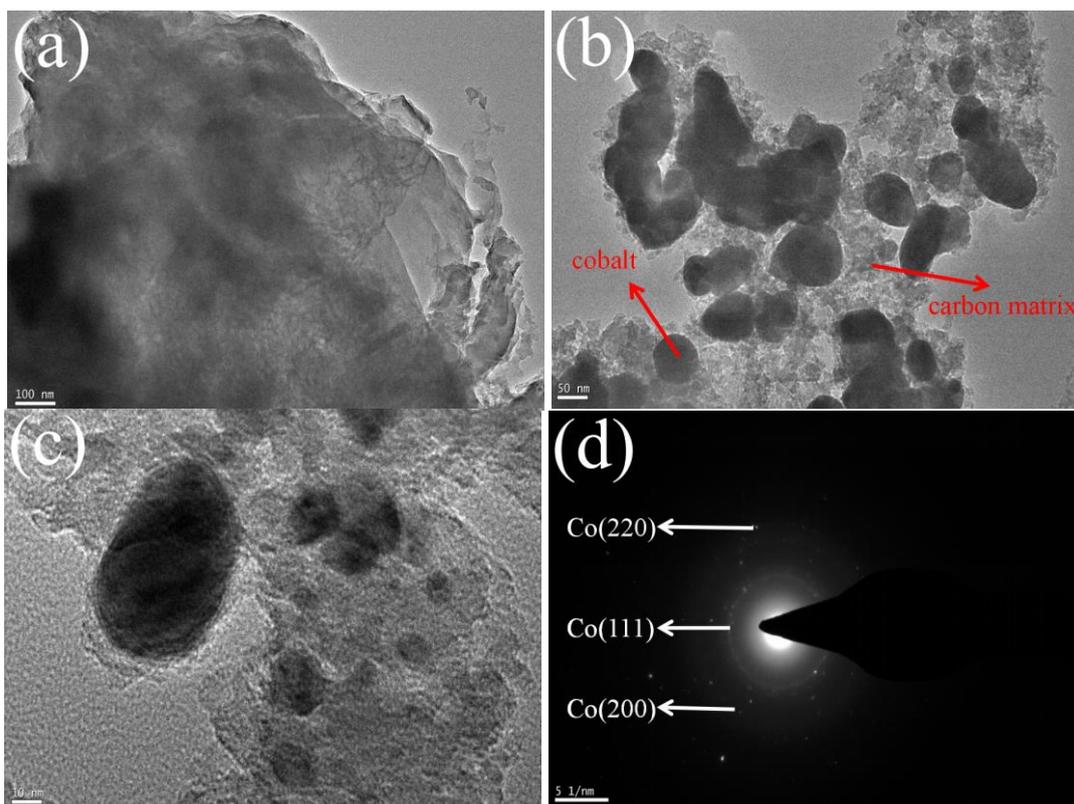
Figure 3. TEM images of C sample(a), Co@C sample (b, c) and SAED pattern of Co@C sample(d)

The TEM images, seen in Figure 3, are used to observe the morphology of the Co@C and C samples. As shown in Figure 3 (a), the pure carbon matrix shows network morphology of lamellar structure. Figure 3(a) shows the lamellar structure of the C samples with smooth carbon planes. Some ripples are also observed on the carbon plane, suggesting disordered stacking of these carbon planes[17]. As shown in Figure 3(b), the cobalt nanoparticles are uniformly embedded in the carbon matrix. A closer look of the Co@C sample reveals a core-shell structure, in which the cobalt nanoparticles are wrapped by carbon films that are formed through the catalysis of cobalt nanoparticles (Figure 3(c))[18]. The selected area electron diffraction (SAED) pattern, seen in Figure 3(d), shows the diffraction rings of the (111), (200), and (220) planes of Co, indicating the well crystallization of cobalt nanoparticles. This is also in agreement with the XRD result. The carbon shell with numerous defects could provide active sites for the formation of SEI film[19]. The anchored cobalt nanoparticles are beneficial to the Li$^+$ migration and the electrical conductivity of carbon matrix[20, 21]. Therefore, the unique structure of the Co@C sample could improve the reversible capacity and rate performance when used as anode materials for LIBs.
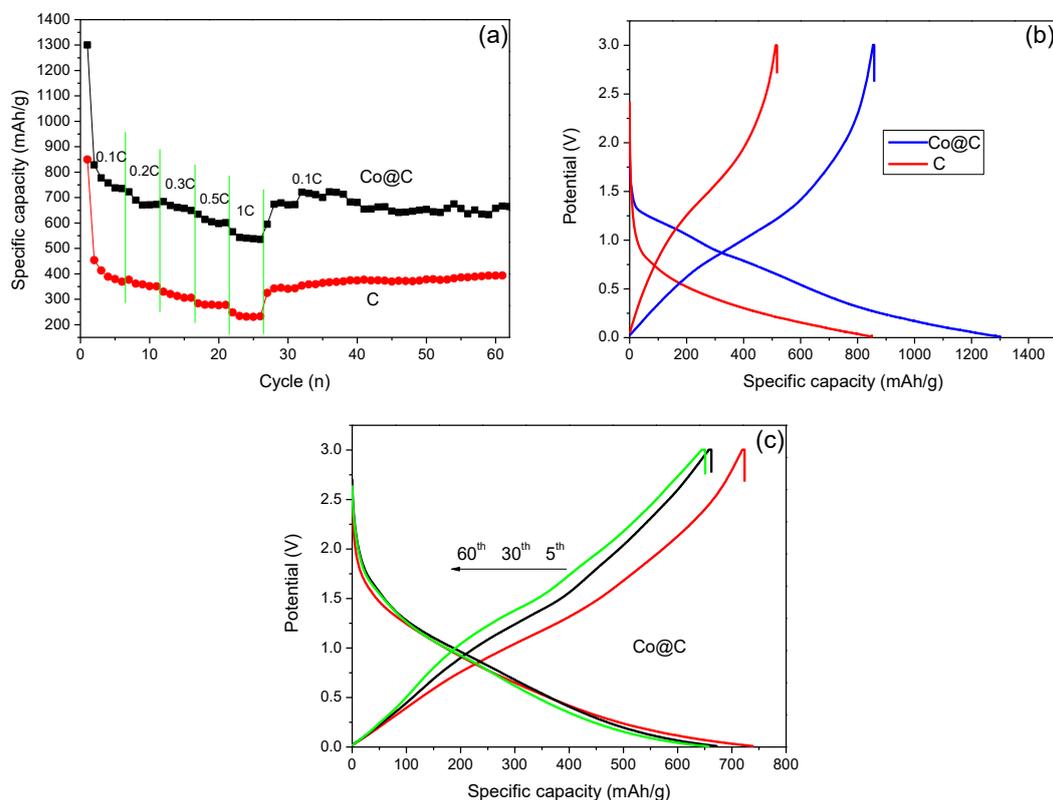
Figure 4. Rate capability of C and Co@C at different current density (a); first charge/discharge curves of C and Co@C (b) and charge/discharge curves of Co@C after different cycles (c)

Figure.4 (a) shows the rate capabilities of the C and Co@C samples. The specific capacities of first cycle for C and Co@C reach 849.8 mAh g^{-1} and 1299.3 mAh g^{-1}, respectively. The specific capacities of the second cycle drop to 453.9 mAh g^{-1} and 828.5 mAh g^{-1}, respectively, owing to the electrolyte decomposition and the formation of SEI films during the charge/discharge process[22]. The

Co@C exhibits specific capacity of 1299.3, 735.2, 673, 648.7, 601.5, and 565.4mAh g^{-1} at different current densities of 0.1C, 0.2C, 0.3C, 0.5C, and 1C (1C=372mA.g^{-1}), respectively. When the current density returns to 0.1C, the Co@C sample still remains a specific capacity of 657.3 mAh g^{-1}, indicating the better rate and cycle performance of Co@C.

From the first charge/discharge curve of C and Co@C, shown in Figure 4(b), the discharge voltage platform increased to ~1.35 V after embedding cobalt nanoparticles in the carbon matrix. This can be attributed to the interaction of cobalt nanoparticles with lithium ions during the charge/discharge process, which is beneficial to the reversible capacity[23]. From the curves in Figure 4(c), it is found that the specific capacities of Co@C are 738.3, 671.8 and 657.3mAh.g^{-1} after 5, 30 and 60 cycles, respectively, revealing the excellent cycle performance of Co@C. The high reversible capacity and excellent cycle performance is attributed to a core-shell structure of Co@C. The embedded cobalt nanoparticles are benefit to the Li^{+} migration and the electronic conductivity of carbon matrix. The strong-bonded carbon shell not only provides active sites of Li^{+} ions, but also reduces the volume effect of cobalt nanoparticles, preventing them from agglomerating during charge/discharge process.
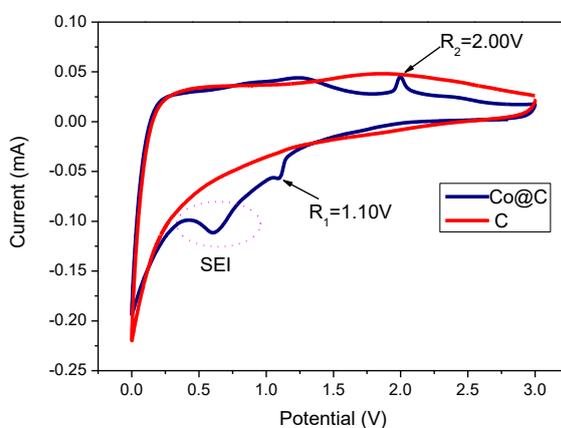
Figure 5. CV profiles of C and Co@C at scan rate of 0.1 mV.s^{-1}

The CV profiles are recorded and used to observe the Li+ ion storage behavior (Figure 5). There are two reduction/oxidation peaks at 0.013 and 0.136 V for the C electrode, owing to the Li+ ion insertion/extraction processes into/from the carbon layers, respectively. The broad peak at near 1.8 V arise from the removal of lithium bounded on the edges of carbon fragments[24]. When the Co@C electrode is used, the electrochemical insertion/extraction behavior of lithium ions is quite different.. The reduction peak at ~0.6 V is attributed to the degradation of the electrolyte and the formation of the solid electrolyte interface (SEI)[25-27]. The broad redox peak at 1.10 V indicates the interaction between Co and Li species at the initial stage of the Li+ intercalation. The oxidation peak at 2.00 V is attributed to the Li+ ion extraction process from the Co@C electrode.
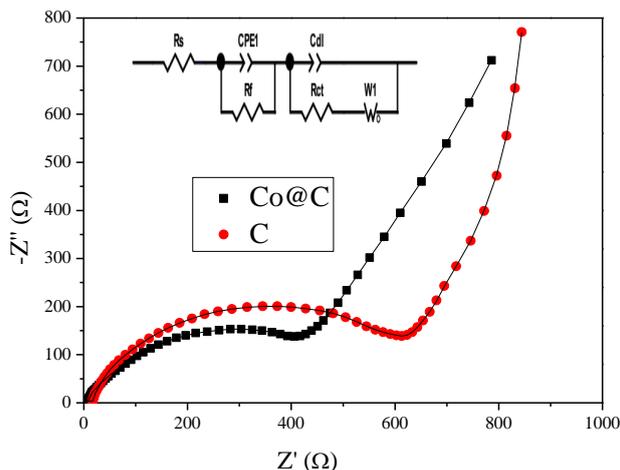
Figure 6. Nyquist plots of C and Co@C

Table 1. The parameters obtained by fitting an equivalent circuit of C and Co@C electrodes

Sample	Rs(Ω)	Rf(Ω)	Rct(Ω)
Co@C	7.4±0.2	27.8±8.6	323.8±14.3

To further understand the reasons for the improved rate capability and cycling stability of Co@C sample, the EIS is performaned and the Nyquist plots of the C and Co@C electrodes are shown in Figure 6. The semicircle diameter of Co@C electrode is smaller than that of the carbon electrode, indicating a smaller surface film resistance and lithium-ion charge transfer resistance. The equivalent circuit is exhibited in the inset. The equivalent analog of Rf relates to the Li+ migration through the surface films[28]. Rs represents the electrolyte resistance and Rct represents the charge transfer resistance of lithium-ion at the interface between electrolyte and electrode. and a sloped line at low frequency is indexed with the Warburg resistance (W1)[29, 30]. The resistances are summarized in Table.1The Rf and Rct of the carbon electrode are 285.3±18.4 and 567.5±27.12, respectively. But for the Co@C electrode, the Rf and Rct drastically reduced to 27.8±8.6 and 323.8±14.3, respectively. The EIS results suggest that the kinetics of Li+ and electronic transport are enhanced by embedding cobalt nanoparticles into the carbon matrix, leading to the excellent electrochemical performance.

Table 2. Comparison of the Co@C electrode with similar electrodes reported in the literature

Material	Grain size	1st discharge capacity(mAh g^{-1})	Cycle number	Current density(mA g^{-1})	Specific capacity(mAh g^{-1})	Ref.
C/Co	10 ~20	1146	40	50	Over 600	[13]
Co/G	100	670.8	120	50	562.4	[31]
CoNC	~100	625	150	500	455.7	[32]
Co@C	~28	1299.3	60	50	657.3	This work

By comparison from Table 2, the discharge capacity of Co@C composite is much higher than other similar materials. In addition, after 40 cycles, Co@C composite also outperforms other similar materials in grain size and cycle stablity.

4. CONCLUSION

Co@C composite was successfully produced by pyrolysing a mixture of ([BMIm]N(CN)$_2$and (Co(AC)·4H$_2$O). A core-shell structure was obtained, in which the cobalt nanoparticles uniformly distributed in the carbon matrix. The cobalt nanoparticles not only provided active sites for lithium storage, but also enhanced the electrical transport and Li$^+$ migration during the charge/discharge process. The carbon shell, with many defects, provided active sites for Li$^+$ ions and also prevented the agglomeration of the cobalt nanoparticles during the charge/discharge process. Due to this unique structure, the Co@C composite delivered a reversible capacity of 657.3mAh g^{-1} after 60 cycles at a current density of 0.1C, which is twice the capacity of the pure carbon matrix. The Co@C electrode also exhibited excellent rate and cycling performances. These results indicate that the Co@C composite can be integrated into highly efficient energy storage applications, which with further optimization should be suitable for widespread applications.

References

1. W. Wei, Z. Wang, Z. Liu, Y. Liu, L. He, D. Chen, A. Umar, L. Guo, J. Li, *J Power Sources*, 238 (2013)376.
2. V.S. Espinoza, S. Erbis, L. Pourzahedi, M.J. Eckelman, J.A. Isaacs, *ACS Sustainable Chemistry & Engineering*, 2 (2014)1642.
3. B. Scrosati, J. Garche, *J Power Sources*, 195 (2010)2419.
4. Y. Jiang, X. Yan, W. Xiao, M. Tian, L. Gao, D. Qu, H. Tang, *J. Alloy. Compd.*, 710 (2017)114.
5. L. Li, G. Zhou, X.-Y. Shan, S. Pei, F. Li, H.-M. Cheng, *J Power Sources*, 255 (2014)52.
6. Y. Ma, J. Huang, X. Liu, F. Bu, L. Wang, Q. Xie, D.-L. Peng, *Chemical Engineering Journal*, 327 (2017)678.
7. X. Wang, S. Dai, *Angew Chem Int Ed Engl*, 49 (2010)6664.
8. S. Zhang, H. Gu, H. Pan, S. Yang, W. Du, X. Li, M. Gao, Y. Liu, M. Zhu, L. Ouyang, D. Jian, F. Pan, *Advanced Energy Materials*, 7 (2017)1601066.
9. X. Zhu, Y. Zhu, S. Murali, M.D. Stoller, R.S. Ruoff, *J Power Sources*, 196 (2011)6473.
10. K. Cao, L. Jiao, Y. Liu, H. Liu, Y. Wang, H. Yuan, *Advanced Functional Materials*, 25 (2015)1082.
11. N. Recham, M. Armand, R. Janot, C. Masquelier, L. Dupont, J.M. Tarascon, *Zeitschrift für anorganische und allgemeine Chemie*, 634 (2008)2005.
12. Y.J. Mai, J.P. Tu, C.D. Gu, X.L. Wang, *J Power Sources*, 209 (2012)1.
13. J.C. Yue, X.Y. Zhao, D.G. Xia, *Electrochem Commun*, 18 (2012)44.

14. D. Zhang, D. Cao, K. Ye, J. Yin, K. Cheng, G. Wang, *Electrochimica Acta*, 139 (2014)250.
15. L. Sun, H. Li, L. Ren, C. Hu, *Solid State Sciences*, 11 (2009)108.
16. E. Duraisamy, P. Gurunathan, H.T. Das, K. Ramesha, P. Elumalai, *J Power Sources*, 344 (2017)103.
17. E.J. Yoo, J. Kim, E. Hosono, H. Zhou, T. Kudo, I. Honma, *Nano Letters*, 8 (2008)2277.
18. H. Zhang, C. Liang, J. Liu, Z. Tian, G. Shao, *Carbon*, 55 (2013)108.
19. F. Béguin, F. Chevallier, C. Vix-Guterl, S. Saadallah, V. Bertagna, J.N. Rouzaud, E. Frackowiak, *Carbon*, 43 (2005)2160.
20. I.R.M. Kottegoda, Y. Kadoma, H. Ikuta, Y. Uchimoto, M. Wakihara, *Electrochemical and Solid-State Letters*, 5 (2002)A275.
21. Y. Wu, C. Jiang, C. Wan, E. Tsuchida, *Electrochem Commun*, 2 (2000)626.
22. L. Wang, Y. Yu, P.C. Chen, C.H. Chen, *Scripta Materialia*, 58 (2008)405.
23. Y.J. Mai, J.P. Tu, C.D. Gu, X.L. Wang, *J. Power Sources*, 209 (2012)1.
24. T. Zheng, W. Mckinnon, J. Dahn, *Journal of the Electrochemical Society*, 143 (1996)2137.
25. D. Xu, C. Mu, J. Xiang, F. Wen, C. Su, C. Hao, W. Hu, Y. Tang, Z. Liu, *Electrochimica Acta*, 220 (2016)322.
26. N.S. Marzuki, N.U. Taib, M.F. Hassan, N.H. Idris, *Electrochimica Acta*, 182 (2015)452.
27. G. Yan, X. Li, Z. Wang, H. Guo, C. Wang, *J. Power Sources*, 248 (2014)1306.
28. M.D.L. And, D. Aurbach, *Journal of Physical Chemistry B*, 101 (1997)4641.
29. M.V. Reddy, T. Yu, C.H. Sow, Z.X. Shen, C.T. Lim, G.V. Subba Rao, B.V.R. Chowdari, *Advanced Functional Materials*, 17 (2007)2792.
30. Z. Yan, Q. Hu, G. Yan, H. Li, K. Shih, Z. Yang, X. Li, Z. Wang, J. Wang, *Chemical Engineering Journal*, 321 (2017)495.
31. G.-C. Li, W. Zhao, *J. Alloy. Compd.*, 716 (2017)156.
32. C. An, M. Wang, W. Li, Q. Deng, Y. Wang, L. Jiao, H. Yuan, *Electrochimica Acta*, 250 (2017)135.